Lung dendritic cells imprint T cell lung homing and promote lung immunity through the chemokine receptor CCR4

Permanent link

http://nrs.harvard.edu/urn-3:HUL.InstRepos:11879883

Share Your Story

The Harvard community has made this article openly available.
Please share how this access benefits you. Submit a story .

Accessibility

Lung dendritic cells imprint T cell lung homing and promote lung immunity through the chemokine receptor CCR4

Zamaneh Mikhak, James P. Strassner, and Andrew D. Luster

Center for Immunology and Inflammatory Diseases, Division of Rheumatology, Allergy, and Immunology, Massachusetts General Hospital, Harvard Medical School, Charlestown, MA 02129

T cell trafficking into the lung is critical for lung immunity, but the mechanisms that mediate T cell lung homing are not well understood. Here, we show that lung dendritic cells (DCs) imprint T cell lung homing, as lung DC–activated T cells traffic more efficiently into the lung in response to inhaled antigen and at homeostasis compared with T cells activated by DCs from other tissues. Consequently, lung DC–imprinted T cells protect against influenza more effectively than do gut and skin DC–imprinted T cells. Lung DCs imprint the expression of CCR4 on T cells, and CCR4 contributes to T cell lung imprinting. Lung DC–activated, CCR4-deficient T cells fail to traffic into the lung as efficiently and to protect against influenza as effectively as lung DC–activated, CCR4-sufficient T cells. Thus, lung DCs imprint T cell lung homing and promote lung immunity in part through CCR4.

CORRESPONDENCE
Zamaneh Mikhak:
mikhak.zamaneh@
mgh.harvard.edu
OR
Andrew D. Luster:
aluster@mgh.harvard.edu

Abbreviations used: 7-AAD, 7-aminoactinomycin D; APC, allophycocyanin; BAL, bronchoalveolar lavage fluid; HI, homing index; LP, lamina propria; MLN, mesenteric LN; PP, Peyer's patch; PTX, pertussis toxin; QPCR, quantitative PCR; SLN, skin-draining LN; TLN, thoracic LN.

CD4^{+} T cells orchestrate the recruitment and subsequent activation of innate and adaptive immune cells in the tissue through the production of cytokines and critically contribute to the generation of a robust immune response to invading pathogens (Reinhardt et al., 2006). A prerequisite for CD4^{+} T cell participation in host defense is their recruitment into peripheral nonlymphoid tissue both in response to pathogens and at homeostasis so that antigen-experienced T cells are positioned where pathogen reencounter is most likely to occur. The mechanisms that govern this strategic distribution of T cells into tissues are not fully defined.

Organs with large epithelial surfaces such as the gut and the skin are in constant contact with the environment and are exposed to potential pathogens on a regular basis and therefore need an efficient immune response strategy to prevent infections at these sites. The unique structure and function of each organ determine its exposures and vulnerabilities to specific pathogens and make reexposure to a particular pathogen more likely in the same organ. For example, by virtue of its ecology, the gut is susceptible to infection with *Salmonella* and *Shigella*, organisms which are not pathogens in the skin. To streamline T cell memory immune responses based on the predictability of pathogen reexposure, the gut and the skin have evolved

tissue-selective T cell imprinting, a process whereby DCs derived from the gut instruct T cells to home preferentially into the gut, whereas DCs derived from the skin instruct T cells to preferentially home into the skin. Gut DCs imprint the expression of $\alpha 4\beta 7$ and CCR9 on T cells, and in doing so enable their entry into the small intestine in response to intestinal MAdCAM-1 and CCL25, respectively (Stagg et al., 2002; Johansson-Lindbom et al., 2003; Mora et al., 2003). Similarly, skin-derived DCs imprint T cell expression of P- and E-selectin ligands and CCR10, allowing T cell skin homing via cutaneous P- and E-selectins and CCL27, respectively (Campbell and Butcher, 2002; Dudda et al., 2004; Sigmundsdottir et al., 2007). This may explain why peripheral blood memory T cells that proliferate in response to rotavirus, a gut pathogen, are $\alpha 4\beta 7^+$ (Rott et al., 1997), whereas peripheral blood T cells specific for herpes simplex virus 2, a skin tropic virus, express high levels of CLA (Koelle et al., 2002). The unique structure and function of each organ also offer a distinct set of tissue-specific autoantigens, such that the autoantigens generated in

the intestine would be different from those generated in the skin. Therefore, tissue-selective T cell imprinting might have also evolved to enable tissue-specific regulatory T cells to home efficiently to the location of their autoantigens.

Tissue-selective T cell imprinting was described a decade ago for the gut and the skin and to date has not been shown for any other organ, raising the possibility that it might be a phenomenon restricted to these two organs. Like the gut and the skin, however, the lung is a large epithelial organ in continuous contact with the environment and potential pathogens. The lung also has its own unique structure and function, specific pathogen susceptibility (i.e., pneumococcus and influenza), and autoantigens and thus is poised to benefit from tissue-selective T cell imprinting. Understanding whether lung DCs imprint T cell lung homing is fundamental to understanding T cell immunity to inhaled antigens and pathogens. Whether lung DCs instruct T cells to home to the lung has implications for vaccine development and potentially opens novel therapeutic approaches for a variety of inflammatory T cell–mediated lung diseases. Here, we sought to determine whether lung DCs imprint T cell lung homing and, if so, the impact of lung imprinting on lung immunity.

RESULTS

Lung DC–activated T cells home efficiently into the lung in response to inhaled antigen

To determine whether lung DCs imprint T cell lung homing, we compared the trafficking of antigen-specific CD4$^+$ T cells activated by lung DCs versus those activated by DCs isolated from other sites into the lung in response to inhaled antigen. Naive C57BL/6 mice were injected with fms-like tyrosine kinase 3 ligand (Flt3L)-secreting melanoma cells to expand DC numbers (Mora et al., 2003). On days 12–14, DCs were isolated from the lung, thoracic LNs (TLNs), spleen, skin-draining LNs (SLNs), mesenteric LNs (MLNs), ear skin, and lamina propria (LP) from the same pool of donor mice, with DC purity >95% (not depicted). DCs were used to activate CD4$^+$ T cells isolated from Thy1.1$^+$ OTII mice, which are transgenic for the TCR recognizing OVA peptide 323–339 (pOVA$_{323–339}$). DC–T cell cultures were established using pOVA$_{323–339}$ without any exogenous cytokines. The use of OVA peptide eliminated the differences in the ability of DCs to take up and/or process antigen as a variable. By not using exogenous cytokines, we did not skew DC–T cell interactions toward any differentiation pathway. On day 6, DC-activated Thy1.1$^+$ OTII cells demonstrated equivalent activation and differentiation (not depicted) before their adoptive transfer into separate naive Thy1.2$^+$ recipient mice. Recipient mice were given three daily aerosolized OVA challenges and bronchoalveolar lavage fluid (BAL), and lungs were harvested 24 h after the last challenge. The number of adoptively transferred CD4$^+$Thy1.1$^+$ cells in each site was compared between recipients of DC-activated T cells.

Lung DC–activated T cells trafficked significantly more efficiently into the BAL and lung compared with TLN, spleen, SLN, MLN, skin, and LP DC–activated T cells (Fig. 1, a and b

[left, BAL: 5-, 4-, 2.6-, 5-, 22-, and 2.6-fold, respectively; right, lung: 3.7-, 3.4-, 2.3-, 3.5-, 5.3-, and 2-fold, respectively]). Because Flt3L does not expand alveolar macrophages (von Wulffen et al., 2007; Hao et al., 2008), we show that the lung DC preparation used in these experiments contained <1% alveolar macrophages defined as autofluorescent CD11c$^+$ cells (Fig. 1 c; Lambrecht and Hammad, 2012). There was no difference in the number of Thy1.1$^+$ OTII cells in the spleen or Peyer's patches (PPs; Fig. 1 d). Consistent with their enhanced lung homing, lung DC–activated T cells induced more inflammation in the lungs of recipient mice compared with skin DC–activated T cells (Fig. 1 e).

To ensure that Flt3L did not cause the lung-homing advantage of lung DC–activated T cells, we repeated these experiments using DCs isolated from mice that were not treated with Flt3L. Because these untreated mice did not have an expanded population of DCs, tissues were pooled from up to 20 mice per experiment to obtain adequate numbers of DCs. Single cell preparations of unexpanded tissues were rested overnight. The next day, nonadherent cells were collected, and CD11c$^+$ cells were isolated with purity >97% (not depicted). After the overnight incubation and exclusion of adherent cells, the percentage of alveolar macrophages in the lung DC preparation of unexpanded mice was 17 ± 4% (not depicted). DCs were used to activate CD4$^+$ T cells in vitro, yielding similar levels of T cell differentiation and activation (not depicted), followed by adoptive transfer experiments as described above. Despite the presence of some alveolar macrophages in the lung DC preparations from unexpanded mice, lung DC–activated T cells trafficked significantly more efficiently into the BAL and lung compared with spleen and SLN DC–activated T cells (Fig. 1 f, left, BAL: 9- and 10-fold, respectively; right, lung: 2.5- and 6.6-fold, respectively).

We saw similar results when we studied antigen-specific CD8$^+$ T cells. DCs from Flt3L–expaned mice were used to activate CD8$^+$ T cells isolated from Thy1.2$^+$ OTI mice, which are transgenic for the TCR recognizing OVA peptide 257–264 (pOVA$_{257–264}$). Adoptive transfer experiments were performed as described above in Thy1.1$^+$ mice. Lung DC–activated OTI cells trafficked significantly more efficiently into the BAL and lung compared with spleen, SLN, and MLN DC–activated OTI cells (Fig. 1 g, left, BAL: 8.6-, 4.4-, and 5.5-fold, respectively; right, lung: 23-, 4-, and 4.4-fold, respectively). These results demonstrate that lung DCs endow T cells with a lung-homing advantage as lung DC–activated T cells were superior in lung homing in response to inhaled antigen.

No difference in proliferation and apoptosis

To assess proliferation in vivo, recipients of DC-activated T cells were given an i.p. dose of BrdU immediately before the third aerosolized OVA challenge, and TLNs were harvested 2 h later (Mikhak et al., 2009). There was no statistically significant difference in the total number of cells in the TLN of recipient mice (not depicted). Furthermore, we observed no difference in the percentage of CD4$^+$Thy1.1$^+$BrdU$^+$ cells in the lymphocyte gate in the TLN in recipients of lung DC– versus
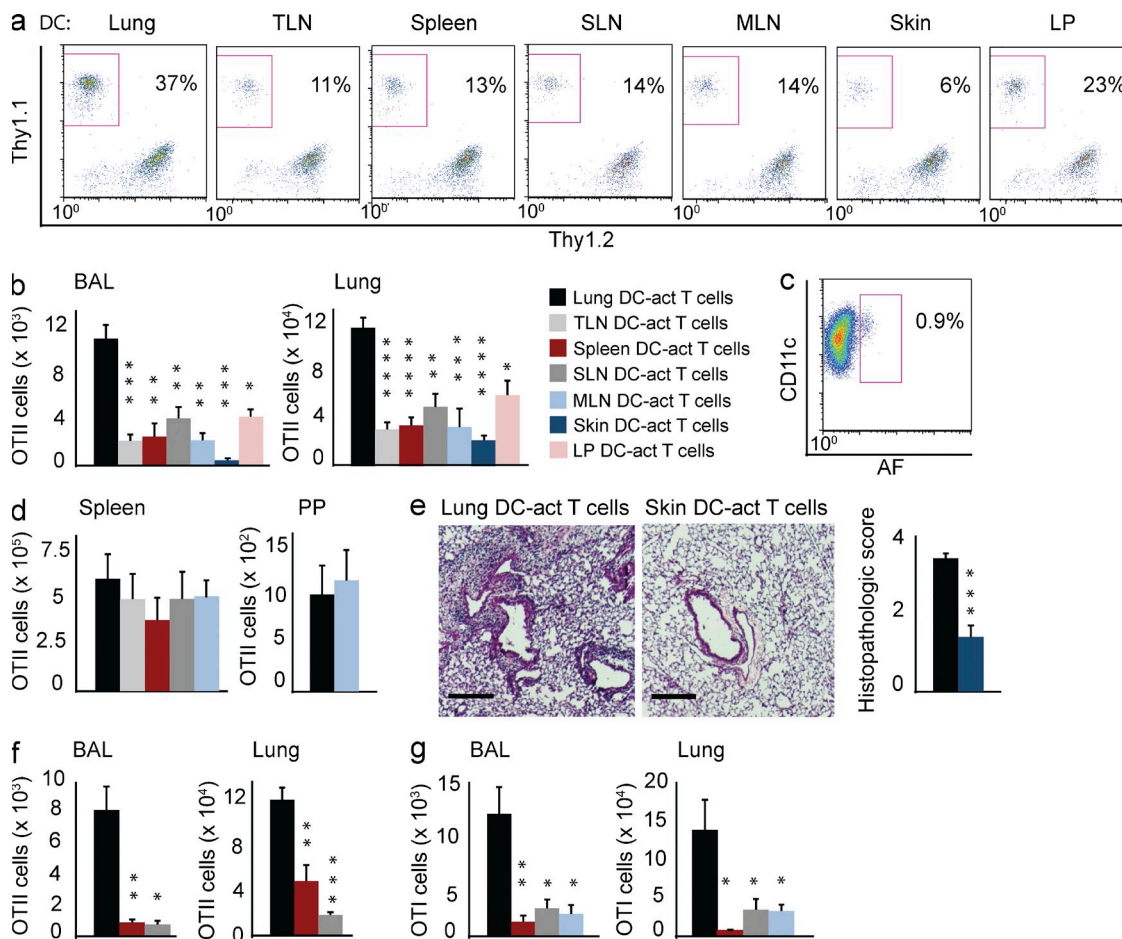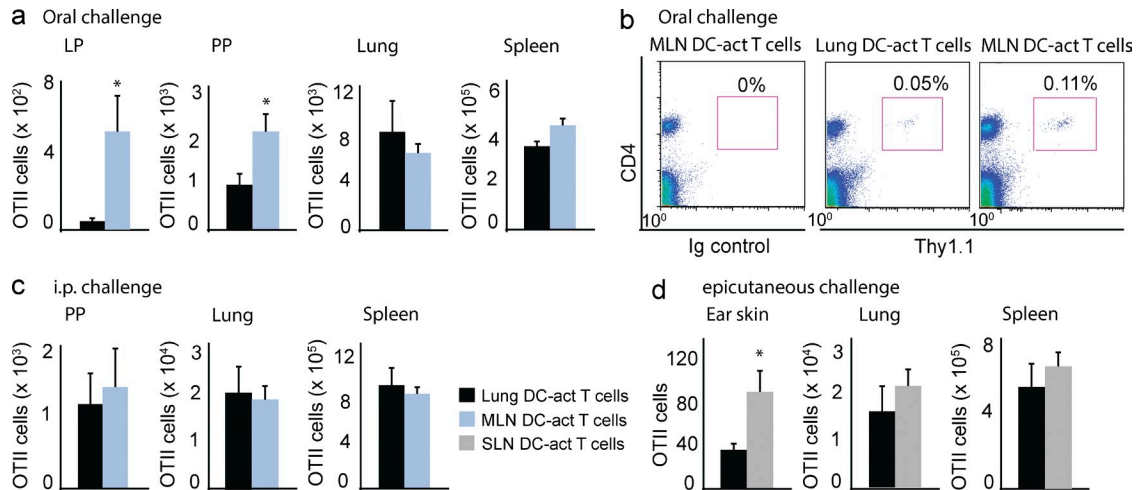
Figure 1. Lung DC–activated T cells home efficiently into the lung in response to inhaled antigen. DCs isolated from Flt3L-expanded C57BL/6 mice were used to activate Thy1.1+ OTII cells in vitro. DC-activated OTII cells were adoptively transferred into separate Thy1.2+ C57BL/6 recipient mice, followed by three inhaled OVA challenges. (a) BAL from recipients of DC-activated OTII cells were analyzed for Thy1.1+ (y axis) versus Thy1.2+ (x axis) expression in the CD4+ gate. (b) Thy1.1+ OTII cells in the BAL and lung from recipients of DC-activated T cells were enumerated 24 h after the last OVA challenge. n = 8–38 mice per group total from 2–10 independent experiments for a and b. P-values are calculated between recipients of lung DC– versus other DC-activated T cells. (c) Flow cytometry of lung DCs isolated from Flt3L-expanded mice gating on live CD11c+ cells, demonstrating the expression of CD11c (y axis) versus auto-fluorescence (AF) in the FITC open channel (x axis). Data are representative of three independent experiments. (d) Thy1.1+ OTII cells in the spleen and PPs from recipients of DC-activated T cells were enumerated. n = 2–3 independent experiments. (e) Lung tissue from recipients of lung DC– versus skin DC–activated OTII cells were stained with H&E and scored by histology. n = 9–10 mice per group total from three independent experiments. Bars, 150 μm. (f) DCs isolated from unexpanded C57BL/6 mice were used to activate Thy1.1+ OTII cells in vitro, which were then adoptively transferred into separate Thy1.2+ C57BL/6 recipient mice, followed by three inhaled OVA challenges. Thy1.1+ OTII cells in the BAL and lung from recipients of DC-activated OTII cells were enumerated. n = 9–23 mice per group total from three to six independent experiments. (g) DCs isolated from Flt3L-expanded C57BL/6 mice were used to activate Thy1.2+ OTI cells in vitro. DC-activated OTI cells were adoptively transferred into separate Thy1.1+ C57BL/6 recipient mice, followed by three inhaled OVA challenges. Thy1.2+ OTI cells in the BAL and lung from recipients of DC-activated OTI cells were enumerated. n = 6–15 mice per group total from two to four independent experiments. *, P < 0.05; **, P < 0.005; ***, P < 0.0005; ****, P < 0.00005. Data are presented as mean (±SEM).

other DC–activated T cells (not depicted). To study apoptosis in vivo, we used 7-aminoactinomycin D (7-AAD) on lung samples obtained 24 h after the third OVA challenge. There was no difference in the percentage of CD4+Thy1.1+ 7-AAD+ cells in the lymphocyte gate in the lung in recipients of lung DC– versus other DC-activated T cells (not depicted). These findings demonstrate that the enhanced accumulation of lung DC–activated T cells in the lung after antigen challenge is not caused by their increased proliferation or decreased apoptosis.

The homing advantage of lung DC–activated T cells in response to antigen is specific to the lung

DC-activated T cells were adoptively transferred into separate naive recipient mice followed by oral, i.p., or epicutaneous OVA challenges. Tissues were harvested 24 h later. MLN DC–activated T cells trafficked 11.6- and 2.2-fold more efficiently into LP and PPs compared with lung DC–activated T cells in response to oral OVA challenge (Fig. 2, a and b). This indicates that the impaired trafficking of MLN DC–activated T cells into the lung and the BAL in response to

Figure 2. The homing advantage of lung DC–activated T cells in response to antigen is specific to the lung. DCs isolated from Flt3L-expanded C57BL/6 mice were used to activate OTII cells in vitro. DC-activated T cells were adoptively transferred into separate recipient mice, followed by oral, i.p., or epicutaneous OVA challenges. DC-activated Thy1.1+ OTII cells were transferred into Thy1.2+ C57BL/6 recipients in a–c. DC-activated Thy1.2+ OTII cells were transferred into Thy1.1+ C57BL/6 recipients in d. (a) Thy1.1+ OTII cells in LP, PPs, lung, and spleen from recipients of lung DC– versus MLN DC–activated T cells were enumerated 24 h after one oral OVA challenge. (b) PPs from recipients of lung DC– versus MLN DC–activated T cells after one oral OVA challenge were analyzed for the expression of CD4+ (y axis) and Thy1.1+ (x axis, right) by flow cytometry. (c) Thy1.1+ OTII cells in PPs, lung, and spleen from recipients of lung DC– versus MLN DC–activated T cells were enumerated 24 h after one i.p. OVA challenge. (d) Thy1.2+ OTII cells in the ear skin, lung, and spleen from recipients of lung DC– versus SLN DC–activated T cells were enumerated 24 h after three daily tape strippings and epicutaneous OVA challenges. n = 12 mice per group total from three independent experiments in a and b for PPs, lung, and spleen. n = 6 mice per group total from two independent experiments in a for LP and in c and d. *, P < 0.05. Data are presented as mean (±SEM).

inhaled antigen was not caused by an overall in vivo functional deficit because these cells were capable of more efficiently trafficking into the gut compared with lung DC–activated T cells after oral antigen challenge. There was no difference in the trafficking of lung and MLN DC–activated T cells into the lung and spleen in response to oral OVA challenge (Fig. 2 a) or into PPs, lung, and spleen in response to i.p. OVA challenge (Fig. 2 c). To increase T cell trafficking into the ear skin to detectable levels, we used tape stripping before each epicutaneous OVA challenge and repeated the procedure once daily for 3 d. SLN DC–activated T cells trafficked 2.5-fold more efficiently into the ear skin compared with lung DC–activated T cells in response to three daily tape strippings and epicutaneous OVA challenges (Fig. 2 d). There was no difference in the trafficking of lung and SLN DC–activated T cells into the lung and spleen in response to epicutaneous OVA challenges (Fig. 2 d). These observations indicate that lung DC–activated T cells do not have a trafficking advantage into all tissues in response to antigen, but instead have a specific homing advantage for the lung. Furthermore, consistent with the published literature showing that T cell imprinting is a flexible process (Mora et al., 2005; Liu et al., 2006; Oyoshi et al., 2011), lung DC–activated T cells appear to lose their lung-homing advantage upon reactivation and reprogramming in gut-draining LNs or SLNs.

Lung-imprinting DCs are migratory DCs

We next examined whether the lung DC subset that imprints T cell lung homing is a migratory DC subset that travels from the lung to the TLN upon exposure to inhaled antigen. We isolated DCs from the lung and TLN of Flt3L-expanded mice either 30 min or 24 h after an intranasal dose of OVA with or without an intranasal dose of CCR7 blocking antibody, which has been shown to diminish lung DC migration to the TLN (not depicted; Fainaru et al., 2005). CCR4 blocking antibody was used as a negative control. DC-activated T cells were adoptively transferred into separate naive recipient mice followed by three aerosolized OVA challenges. Lung DC–activated T cells trafficked 2.7-fold more efficiently into the lung compared with TLN DC–activated T cells when DCs were isolated 30 min after intranasal OVA before there was enough time for lung DC migration to the TLN. However, when DCs were isolated 24 h after intranasal OVA, which provided sufficient time for lung DC migration to the TLN (Vermaelen et al., 2001), there was no difference in the trafficking of lung DC– and TLN DC–activated T cells into the lung. In contrast, when DC migration from the lung to the TLN was inhibited by the concurrent treatment of the mice with a CCR7 blocking antibody, TLN DC–activated T cells had a 2.3-fold trafficking defect into the lung (Fig. 3). This was not seen when mice were concurrently treated with a CCR4 blocking antibody (Fig. 3). The intranasal CCR7 and CCR4 blocking antibodies did not adversely affect lung DCs as lung DCs remained fully capable of activating T cells and imprinting lung homing. These data collectively suggest that the lung DC subset that imprints T cell lung homing is a migratory subset that travels from the lung to the TLN upon exposure to inhaled antigen.
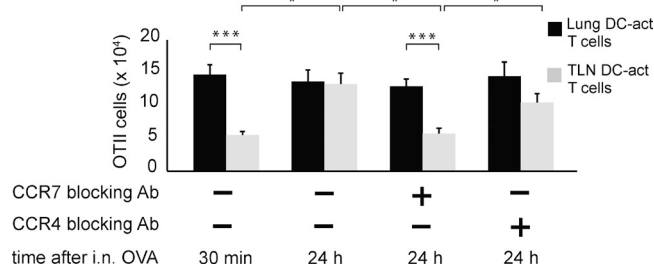
Figure 3. Lung-imprinting DCs are migratory DCs. Lung and TLN DCs isolated from Flt3L-expanded C57BL/6 mice 30 min or 24 h after intranasal OVA with or without intranasal CCR7 or CCR4 blocking antibody were used to activate Thy1.1^{+} OTII cells in vitro. DC-activated T cells were adoptively transferred into separate Thy1.2[+] recipient C57BL/6 mice, followed by three inhaled OVA challenges. Thy1.1^{+} OTII cells in the lung from recipients of lung DC– versus TLN DC–activated T cells were enumerated when DCs were isolated either 30 min or 24 h after intranasal OVA exposure. n = 7–20 mice per group total from two to five independent experiments. *, $P < 0.05$; ***, $P < 0.0005$. Data are presented as mean ($\pm$SEM).

Lung DC–activated T cells home more efficiently into the lung at homeostasis

We next determined whether lung DC–activated T cells exhibit enhanced lung homing at baseline in the absence of antigen. Lung, MLN, and SLN DC–activated T cells were adoptively transferred into separate naive mice without OVA challenges. 72 h after adoptive transfer, lung DC–activated T cells accumulated more efficiently in the BAL and lung of recipient mice compared with MLN and SLN DC–activated T cells (Fig. 4 a, left, BAL: 4.8- and 3-fold, respectively; right, lung, 2.4-fold).

To verify the lung-homing advantage of lung DC–activated T cells at homeostasis, we used competitive adoptive transfer experiments in the absence of antigen and assessed T cell lung homing at a shorter time point, 4 h after adoptive transfer. Lung DC–activated T cells were labeled with CFSE, whereas MLN and SLN DC–activated T cells were separately labeled with orange-fluorescent tetramethylrhodamine (CMTMR). CFSE-labeled, lung DC–activated T cells were mixed with CMTMR-labeled, MLN or SLN DC–activated T cells at 1:1 ratio and adoptively transferred via the tail vein into naive recipient mice. The ratio of input cells was determined using flow cytometry before adoptive transfer. 4 h after adoptive transfer, the percentage of CFSE^{+} and CMTMR^{+} cells was determined in the 7-AAD^{–}CD4^{+} gate within the lymphocyte gate in the lung, spleen, PPs, and SLNs. Homing index (HI) was calculated as $[CFSE^+/CMTMR^+]_{tissue}/[CFSE^+/CMTMR^+]_{input}$ (Mora et al., 2003). Statistical significance was determined against spleen HI. Similar results were obtained when dyes were switched.

After cotransfer of lung and MLN DC–activated T cells, lung DC–activated T cells demonstrated a threefold lung homing advantage over MLN DC–activated T cells (HI = 3 $\pm$ 0.4). There was no difference in spleen homing (HI = 1.1 $\pm$ 0.03). Surprisingly, lung and MLN DC–activated T cells showed similar homing into PPs (HI = 1.1 $\pm$ 0.05), whereas

lung DC–activated T cells homed better into SLNs (HI = 1.4 $\pm$ 0.14; Fig. 4, b [left] and c [top]). After cotransfer of lung and SLN DC–activated T cells, lung DC–activated T cells showed a modest lung-homing advantage over SLN DC–activated T cells (HI = 1.5 $\pm$ 0.06). There was no difference in spleen homing (HI = 1.0 $\pm$ 0.05). Lung DC–activated T cells homed more efficiently into PPs (HI = 1.4 $\pm$ 0.08), whereas lung and SLN DC–activated T cells showed similar homing into SLNs (HI = 0.9 $\pm$ 0.07; Fig. 4, b [right] and c [bottom]). Cumulatively, these results suggest that although lung DC–activated T cells have a lung-homing advantage, they maintain their ability to distribute into the gut and the skin at homeostasis.
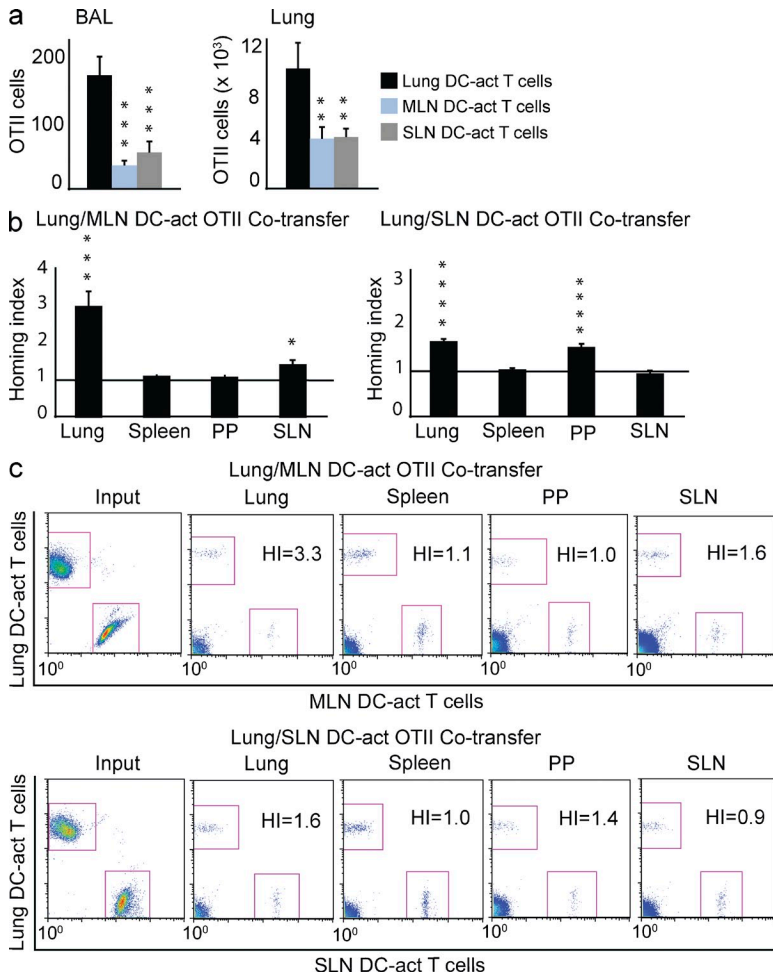
Expression of trafficking molecules by lung DC–activated T cells

We determined that lung homing of lung DC–activated T cells was pertussis toxin (PTX) sensitive as PTX-treated lung DC–activated T cells had a significant trafficking defect into the BAL and lung after aerosolized OVA challenges (Fig. 5 a). To explain the trafficking patterns of lung DC–activated T cells, we next compared the expression of trafficking molecules on the surface of lung DC– versus MLN and SLN DC–activated T cells using flow cytometry on day 5 of culture, a day before their adoptive transfer. 42% ($\pm$5) of lung DC–activated T cells expressed CCR4, whereas only 21% ($\pm$3) of MLN DC–activated T cells were CCR4^{+}. The expression of CCR4 on SLN DC–activated T cells was intermediate (32 $\pm$ 5%) between lung and MLN DC–activated T cells (Fig. 5, b and c). 56% ($\pm$5) of MLN DC–activated T cells expressed $\alpha4\beta7$, whereas only 29% ($\pm$4) of SLN DC–activated T cells were $\alpha4\beta7^+$. The expression of $\alpha4\beta7$ on lung DC–activated T cells was intermediate (40 $\pm$ 6%) between MLN and SLN DC–activated T cells (Fig. 5, c and d). CCR9 expression on lung and SLN DC–activated T cells was lower than that of MLN DC–activated T cells (Fig. 5, c and d, four- and eightfold lower, respectively). 32% ($\pm$2) of SLN DC–activated T cells and 31% ($\pm$1) of lung DC–activated T cells expressed E-selectin ligand, whereas only 19% ($\pm$2) of MLN DC–activated T cells were E-selectin ligand[+] (Fig. 5, c and d). All other trafficking molecules tested were expressed at similar levels by lung, MLN, and SLN DC–activated T cells (Fig. 5 e).

Consistent with the published literature (Kallinich et al., 2005; Thomas et al., 2007; Purwar et al., 2011), we noted CCR4 expression on 24% ($\pm$4) of CD4^{+} T cells in the naive lung, whereas expression levels were low for $\alpha4\beta7$, CCR9, and E-selectin ligand (Fig. 5 f). Because CCR4 was the only trafficking molecule that was differentially expressed on lung DC–activated T cells and was also expressed on a considerable percentage of lung-resident CD4^{+} T cells, we set out to determine the role of CCR4 in the lung-homing advantage of lung DC–activated T cells.

CCR4 contributes to the lung-homing advantage of lung DC–activated T cells

We first determined whether the ligands for CCR4 were expressed in the lung to direct the trafficking of CCR4^{+} T cells.

a BAL / Lung

b Lung/MLN DC-act OTII Co-transfer / Lung/SLN DC-act OTII Co-transfer

**c** Lung/MLN DC-act OTII Co-transfer / Lung/SLN DC-act OTII Co-transfer

Figure 4. Lung DC–activated T cells home efficiently into the lung at homeostasis. DCs isolated from Flt3L-expanded C57BL/6 mice were used to activate Thy1.1+ OTII cells in vitro. DC-activated T cells were adoptively transferred into separate recipient Thy1.2+ C57BL/6 mice without OVA challenges. (a) Thy1.1+ OTII cells in the BAL and lung from recipients of DC-activated T cells were enumerated 72 h after adoptive transfer. $n = 9$ mice per group total from three independent experiments. (b and c) DCs were isolated from Flt3L-expanded mice. CFSE-labeled, lung DC–activated T cells and CMTMR-labeled, MLN DC– or SLN DC–activated T cells were mixed 1:1 and adoptively transferred into recipient mice without OVA challenges. (b) HI (y axis) for the lung, spleen, PPs, and SLNs (x axis) was determined 4 h after competitive adoptive transfer of lung DC– and MLN DC–activated T cells (left; $n = 9$ mice total from three independent experiments) and lung DC– and SLN DC–activated T cells (right; $n = 9$ mice total from three independent experiments). Gating on 7-AAD−CD4+ cells within the lymphocyte gate, HI was calculated as $[CFSE^+/CMTMR^+]_{tissue}/[CFSE^+/CMTMR^+]_{input}$. P-values are calculated between the HI for any tissue versus the HI for spleen. (c) CFSE+ lung DC–activated T cells (y axis) versus CMTMR+ MLN DC (x axis, top)– or SLN DC–activated T cells (x axis, bottom) were analyzed, demonstrating input cells and gated cells in the lung, spleen, PPs, and SLNs. *, $P < 0.05$; **, $P < 0.005$; ***, $P < 0.0005$; ****, $P < 0.00005$. Data are presented as mean (±SEM).

Using quantitative PCR (QPCR), we found high expression levels of CCR4 ligands CCL17 and CCL22 in the lungs of naive mice (Fig. 6 a) compared with the ligands for CCR6 (CCL20) and CXCR3 (CXCL9 and CXCL10), two other chemokine receptors expressed on a considerable percentage of lung–resident T cells. Using immunohistochemistry with a CCL17 monoclonal antibody, we found that CCL17 was expressed in both airway epithelial cells as well as the luminal aspect of endothelial cells in the lungs of naive mice (Fig. 6 b, middle) and in the lungs of mice that received lung DC–activated T cells and three aerosolized OVA challenges (Fig. 6 b, right).

To delineate the functional role of CCR4 in T cell lung imprinting, we first used a competitive adoptive transfer model and asked whether CCR4 deficiency would diminish the lung-homing advantage of lung DC–activated T cells at homeostasis. DCs were isolated from the lung, MLNs, and SLNs of Flt3L-expanded mice and used to activate OTII and CCR4−/− OTII cells in vitro. Lung DC–activated OTII and CCR4−/− OTII cells were labeled separately with CFSE, whereas SLN and MLN DC–activated OTII and CCR4−/− OTII cells were labeled separately with CMTMR. Competitive adoptive transfer experiments were performed as in Fig. 4. Similar results

were obtained when dyes were switched. The HI into the lung after the cotransfer of lung and MLN DC–activated CCR4−/− OTII cells was 1.6 (±0.06), a significant decrease from the HI into the lung after the cotransfer of lung and MLN DC–activated OTII cells (2.8 ± 0.3). The HI into the lung after the cotransfer of lung and SLN DC–activated CCR4−/− OTII cells was 1.4 (±0.08), which was not significantly different from the HI into the lung after the cotransfer of lung and SLN DC–activated OTII cells (1.6 ± 0.07; Fig. 6 c). Therefore, CCR4 deficiency diminished the lung-homing advantage of lung DC–activated T cells over MLN DC–activated T cells but not SLN DC–activated T cells.

We next investigated the functional role of CCR4 in T cell lung imprinting in response to inhaled antigen. Lung DC–activated, Thy1.2+ OTII and CCR4−/− OTII T cells were generated in vitro and adoptively transferred into separate naive Thy1.1+ recipient mice, followed by three daily aerosolized OVA challenges. Lung DC–activated OTII cells trafficked 4.6- and 1.9-fold more efficiently into the BAL and lung, respectively, compared with lung DC–activated CCR4−/− OTII cells (Fig. 6 d). These data collectively demonstrate a functional role for CCR4 in lung DC imprinting of T cell lung homing.
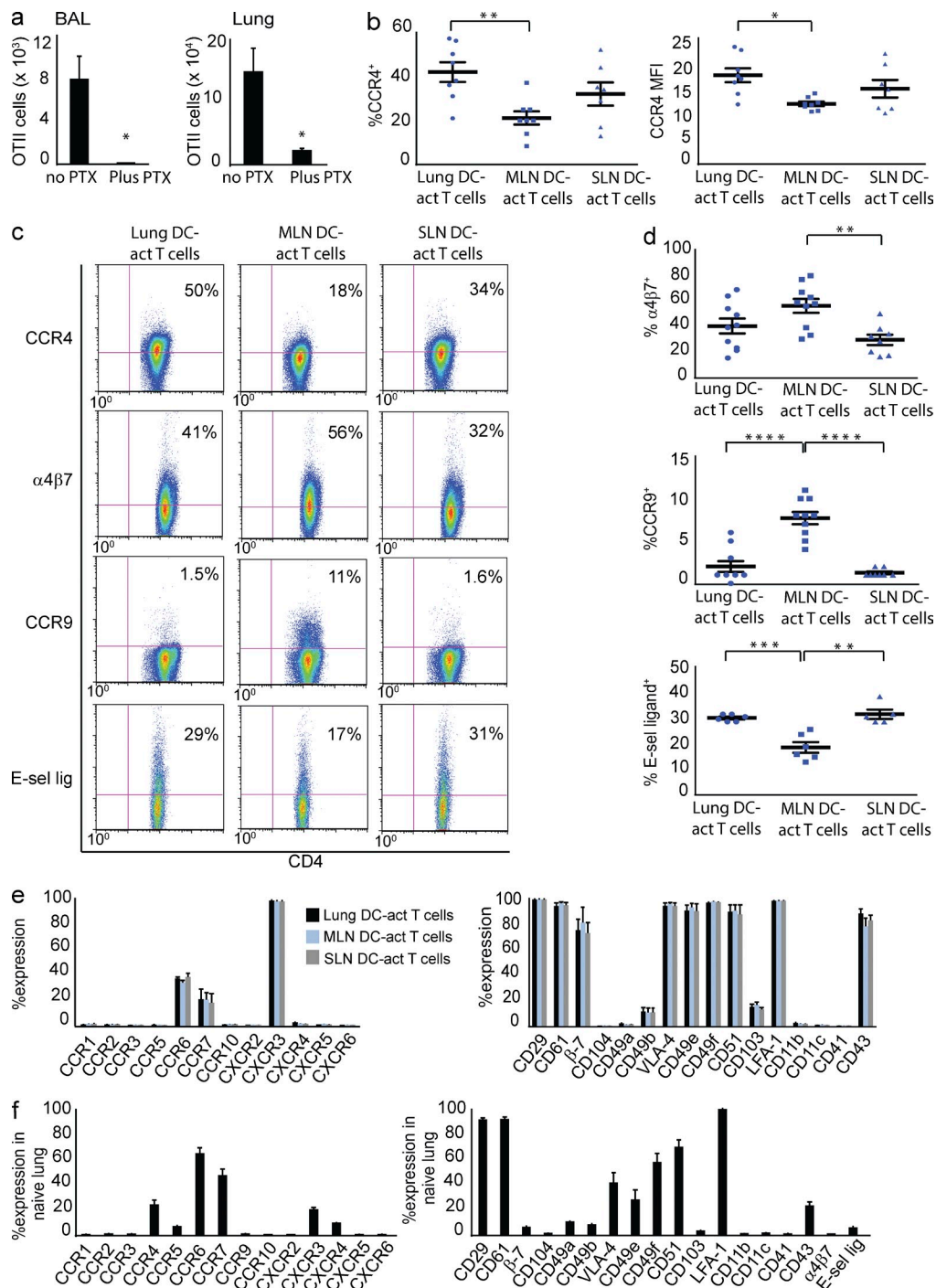
Figure 5. Expression of trafficking molecules by lung DC–activated T cells. DCs isolated from Flt3L-expanded C57BL/6 mice were used to activate OTII cells in vitro in a–e. (a) Thy1.1[+] DC-activated OTII cells were either treated or untreated with PTX and adoptively transferred into Thy1.2[+] recipient mice, followed by three inhaled OVA challenges. Thy1.1^{+} OTII cells were enumerated in the BAL and lung from recipients of PTX-treated or untreated, lung DC–activated T cells. n = 6 mice per group total from two independent experiments. (b–e) DC-activated T cells were analyzed for expression of trafficking molecules on day 5. (b) Percentage (left) and mean fluorescence intensity (MFI; right) of CCR4^{+} lung DC–, MLN DC–, and SLN DC–activated T cells. n = 8 independent experiments. (c) Flow cytometry of lung DC–, MLN DC–, and SLN DC–activated T cells demonstrating the expression of CD4 (x axis) versus CCR4 (top row), $\alpha4\beta7$ (second row), CCR9 (third row), and E-selectin ligand (bottom row; y axis). (d) Percentage of $\alpha4\beta7^+$ (top), CCR9^{+} (middle), and E-selectin ligand[+] (bottom) lung DC–, MLN DC–, and SLN DC–activated T cells. n = 6–10 separate cultures. (e) Percent expression of chemokine receptors (left) and integrins and selectin ligands (right) by lung DC–, MLN DC–, and SLN DC–activated T cells. n = 4–8 independent experiments. (f) Percent expression of chemokine receptors (left) and integrins and selectin ligands (right) by CD4^{+} T cells in the lymphocyte gate in lungs isolated from naive C57BL/6 mice. n = 3–10 individual lungs. *, $P < 0.05$; **, $P < 0.005$; ***, $P < 0.0005$; ****, $P < 0.00005$. Data are presented as mean ($\pm$SEM).
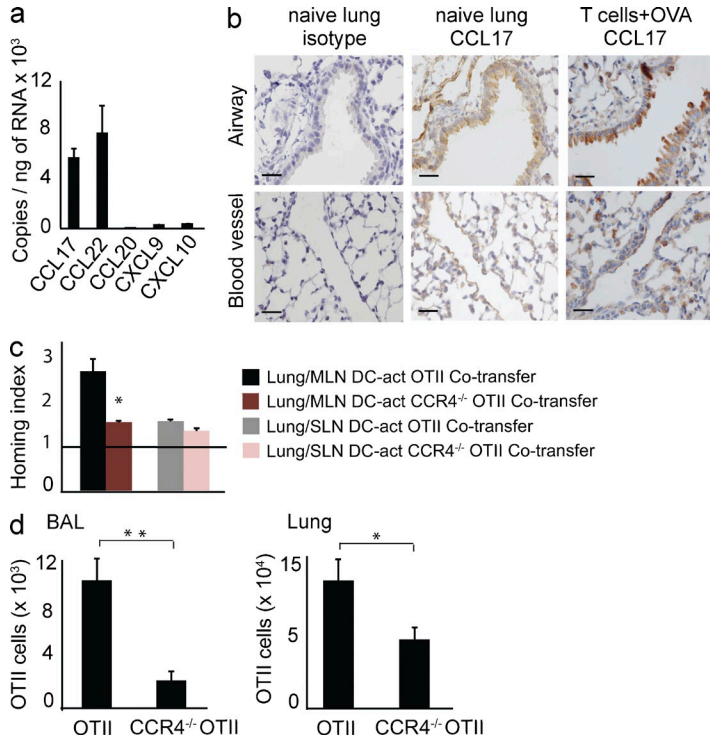
Figure 6. CCR4 contributes to the lung-homing advantage of lung DC-activated T cells. (a) RNA expression of CCR4 (CCL17 and CCL22), CCR6 (CCL20), and CXCR3 ligands (CXCL9 and CXCL10) in lungs of naive C57BL/6 mice. n = 8 mice. (b) Immunohistochemistry staining with CCL17 antibody (middle and right) or isotype control antibody (left) in lungs of naive mice (left and middle) and mice that received lung DC-activated OTII cells, followed by three daily inhaled OVA challenges (right), demonstrating CCL17 expression by both epithelial (top) and endothelial cells (bottom). Staining with the isotype control antibody in the lungs of mice that received OTII cells and OVA was similar to that of naive mice (not depicted). n = 13 samples from three independent experiments. Bars, 20 µm. (c) Lung HI. DCs isolated from Flt3L-expanded mice were used to activate OTII and CCR4$^{-/-}$ OTII cells. CFSE-labeled, lung DC-activated CCR4$^{-/-}$ OTII cells and CMTMR-labeled, MLN DC- or SLN DC-activated CCR4$^{-/-}$ OTII cells were mixed 1:1 and adoptively transferred into recipient C57BL/6 mice without OVA challenges. CFSE-labeled, lung DC-activated OTII cells and CMTMR-labeled, MLN DC- or SLN DC-activated OTII cells were also mixed 1:1 and adoptively transferred into another set of recipient C57BL/6 mice without OVA challenges. Gating on 7-AAD^{-}CD4^{+} cells within the lymphocyte gate, HI for the lung at 4 h after cotransfer was calculated as [CFSE^{+}/CMTMR^{+}]$_{lung}$/[CFSE^{+}/CMTMR^{+}]$_{input}$. P-values are calculated between the HIs for the lung after the competitive transfer of CCR4$^{-/-}$ OTII cells versus OTII cells. n = 6–13 mice total from two to four independent experiments. (d) Lung DCs isolated from Flt3L-expanded mice were used to activate Thy1.2^{+} OTII and CCR4$^{-/-}$ OTII cells. Lung DC-activated OTII and CCR4$^{-/-}$ OTII cells were adoptively transferred into separate Thy1.1^{+} recipient mice, followed by three inhaled OVA challenges. Thy1.2^{+} OTII cells in the BAL and lung of recipient mice were enumerated 24 h after the last OVA challenge. n = 9 mice per group total from three independent experiments. *, P < 0.05; **, P < 0.005. Data are presented as mean (±SEM).

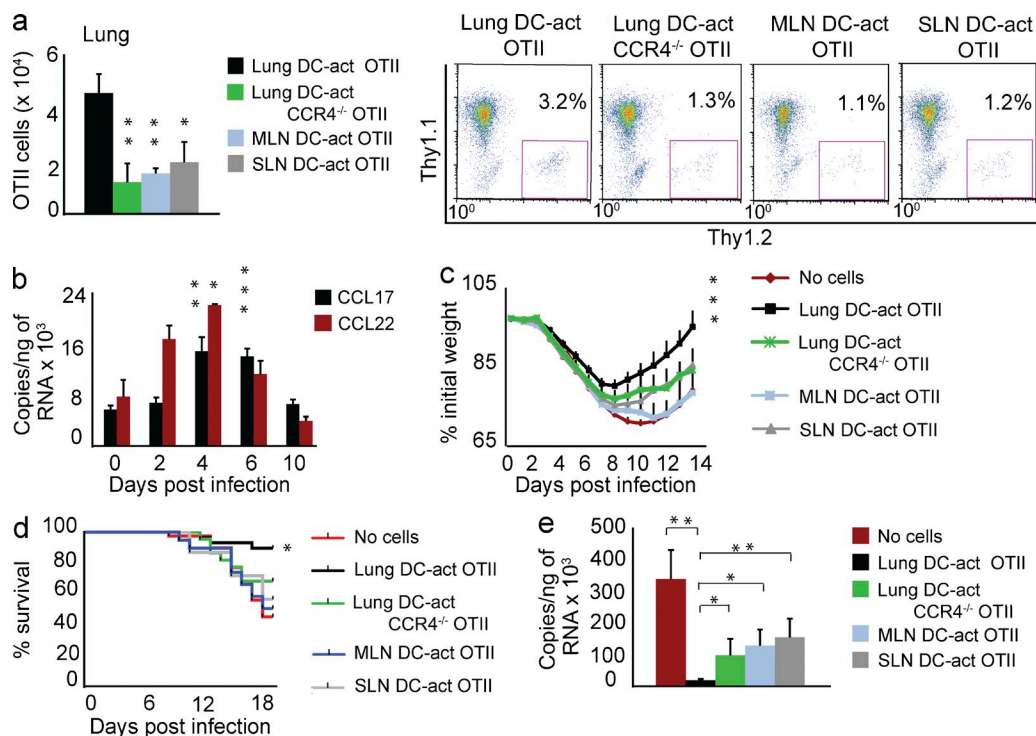## Lung DC–activated T cells protect against influenza

To determine the functional consequence of lung imprinting, we examined whether the enhanced accumulation of lung DC–activated T cells in the lung promoted lung immunity. We used a PR8-H1N1 strain of influenza that expresses pOVA$_{323–339}$ in the hemagglutinin molecule (H1ova; Thomas et al., 2006) and studied the trafficking of CD4^{+} OTII T cells in the context of this infection when T cells were activated by lung DCs versus other DCs. To further delineate the role of CCR4 in lung imprinting, we also compared the trafficking of lung DC–activated OTII and CCR4$^{-/-}$ OTII T cells in response to infection with H1ova. Lung, MLN, and SLN DC–activated Thy1.2^{+} OTII cells and lung DC–activated Thy1.2^{+} CCR4$^{-/-}$ OTII cells were generated in vitro and adoptively transferred into separate naive Thy1.1^{+} recipient mice that were rested for 72 h and then infected with 10^{5} PFU of H1ova intranasally. Lungs were harvested 72 h after infection, and the number of CD4^{+}Thy1.2^{+} T cells was determined. Lung DC–activated OTII cells trafficked 3-, 2.4-, and 3.8-fold more efficiently into the lung in response to intranasal H1ova compared with MLN DC–activated OTII cells, SLN DC–activated OTII cells, and lung DC–activated CCR4$^{-/-}$ OTII cells, respectively (Fig. 7 a). Consistent with the trafficking defect of lung DC–activated CCR4$^{-/-}$ OTII cells, we found that the mRNA levels of the CCR4 ligands CCL17 and CCL22 were increased in the lung upon infection with influenza with an early peak at 4 d after infection (Fig. 7 b). P-values are calculated between any given day and day 0. Recipients of lung DC–activated OTII cells lost weight until day 7 after infection, dropping 19 ± 2% of their original weight. Recipients of no cells and MLN DC–activated OTII cells continued to lose weight until day 11 after infection and showed a weight loss of 30 ± 1% and 28 ± 4%, respectively. Recipients of SLN DC–activated OTII cells and lung DC–activated CCR4$^{-/-}$ OTII cells had an intermediate response to infection as they lost weight until day 8 after infection and decreased their weight by 25 ± 2% and 23 ± 2%, respectively (Fig. 7 c). 90% of recipients of lung DC–activated OTII cells survived, whereas only 47%, 53%, 58%, and 70% of recipients of no cells, MLN DC–activated OTII cells, SLN DC–activated OTII cells, and lung DC–activated CCR4$^{-/-}$ OTII cells survived infection with H1ova, respectively (Fig. 7 d). Finally, recipients of lung DC–activated OTII cells cleared their infection by day 10, consistent with their more rapid weight gain at this time point, whereas recipients of no cells, MLN DC–activated OTII cells, SLN DC–activated OTII cells, and lung DC–activated CCR4$^{-/-}$ OTII cells continued to harbor the influenza virus (Fig. 7 e). These data collectively demonstrate that lung DCs promote lung immunity by imprinting T cell lung homing in part through CCR4.

DISCUSSION

We show that lung DCs imprint T cell lung homing as lung DC–activated T cells were superior in lung homing compared with other DC-activated T cells both in response to inhaled antigen and at homeostasis. Lung DCs imprinted lung-specific

Figure 7. **Lung DC–activated T cells protect against influenza.** DCs isolated from Flt3L-expanded mice were used to activate Thy1.2+ OTII or CCR4$^{-/-}$ OTII cells in vitro. DC-activated T cells were adoptively transferred into separate Thy1.1+ C57BL/6 recipient mice. 72 h after adoptive transfer, mice were infected intranasally with 10^5 PFU of a live OVA$_{323-339}$ expressing PR8-H1N1 influenza virus (H1ova). Lungs were harvested 72 h after infection for analysis. (a, left) Number of Thy1.2+ OTII cells in the lung from recipients of DC-activated T cells infected with H1ova. n = 5–8 mice per group in two independent experiments. P-values are calculated between recipients of lung DC-activated OTII cells versus other groups. (right) Lung flow cytometry from recipients of DC-activated T cells infected with H1ova, demonstrating Thy1.1+ (y axis) versus Thy1.2+ (x axis) cells in the CD4+ gate within the lymphocyte gate. (b) RNA expression of CCL17 and CCL22 in the lungs of mice that were infected with H1ova. n = 6–14 mice per time point in three independent experiments. (c–e) Recipients of either no cells or lung, MLN, or SLN DC–activated OTII cells or lung DC–activated CCR4$^{-/-}$ OTII cells were infected with H1ova as in a. n = 16–42 mice per group total from 4–11 independent experiments for c and d. n = 5–13 mice per group total from four independent experiments for e. (c) Percentage of original weight versus days after infection. (d) Percentage of surviving mice versus days after infection. (e) Viral RNA copies for the polymerase gene of the PR8 influenza virus in the lungs at day 10 after infection. *, $P < 0.05$; **, $P < 0.005$; ***, $P < 0.0005$. Data for a–e are presented as mean ($\pm$SEM).

homing on CD4+ T cells because lung DC–activated T cells had a homing advantage only into the lung. Lung DC–activated T cells did not home more efficiently into the gut compared with MLN DC–activated T cells in response to oral antigen, and they did not home more efficiently into the skin compared with SLN DC–activated T cells in response to epicutaneous antigen.

We demonstrate that lung DC imprinting promotes lung immunity. Lung DC–activated T cells trafficked 3- to 2.4-fold more efficiently into the lung in response to pulmonary infection with influenza compared with MLN and SLN DC–activated T cells, respectively. This enhanced lung homing allowed lung DC–activated T cells, in turn, to provide greater protection against influenza compared with gut and skin DC–activated T cells. Recipients of lung DC–activated T cells lost less weight (19 vs. 25–30%) over a shorter duration (7 vs. 8–11 d) and demonstrated greater survival (90 vs. 47–58%) compared with recipients of no cells or MLN or SLN DC–activated T cells. Finally, mice that received lung DC–activated

T cells cleared the influenza virus by day 10 after infection, whereas recipients of no cells, MLN DC–activated T cells, or SLN DC–activated T cells still harbored the virus at this time. These data delineate the functional consequence of lung DC imprinting and have direct implications for vaccine development against influenza, a significant global public health problem. The overall efficacy of seasonal influenza vaccination was only 56% in the US in 2012–2013 (Centers for Disease Control and Prevention [CDC], 2013), clearly indicating the need for more effective approaches to vaccinate against influenza. Our data suggest that inhalational delivery of a vaccine against influenza might lead to greater protection against the virus. In fact, the live attenuated influenza vaccine, which is delivered intranasally, has been shown to be more efficacious in children aged 6 mo to 7 yr compared with the trivalent inactivated vaccine, which is administered intramuscularly (Osterholm et al., 2012). Furthermore, IFN-γ–producing, influenza-responsive memory T cells are detected after vaccination with the intranasal live attenuated influenza vaccine but not the intramuscular

trivalent inactivated vaccine in children 6–35 mo old (Hoft et al., 2011). These clinical differences could stem from the fact that one vaccine is live attenuated whereas the other is killed and inactivated, but based on our data, it could also result from differences in the route of exposure.

We show that lung DCs imprint T cell lung homing in part through CCR4. First, lung DCs imprint higher levels of CCR4 on CD4$^+$ T cells compared with gut DCs. This observed differential is consistent with the published literature (Dudda et al., 2004; Mora et al., 2005), which demonstrates that retinoic acid down-regulates CCR4 mRNA expression (Iwata et al., 2004). Second, the ligand for CCR4, CCL17, is expressed by epithelial cells (Kawasaki et al., 2001) and on the luminal aspect of endothelial cells both in the lungs of naive mice and mice that were given lung DC–activated T cells and inhaled antigen challenges. Third, the lung-homing advantage of lung DC–activated T cells at homeostasis is proportional to their differential level of CCR4 expression with a 3-fold lung homing advantage compared with MLN DC–activated T cells, which express the lowest levels of CCR4, and a 1.6-fold lung-homing advantage compared with SLN DC–activated T cells, which express intermediate levels of CCR4. We show that CCR4 deficiency decreased the lung-homing advantage of lung DC–activated T cells over MLN DC–activated T cells at homeostasis. Fourth, CCR4 deficiency also compromised the trafficking of lung DC–activated T cells into the BAL and lung in response to inhaled antigen (4.6- and 1.9-fold, respectively). Fifth, and perhaps most importantly, CCR4-deficient, lung DC–activated T cells showed a 3.8-fold decrease in trafficking into the lung in response to pulmonary infection with influenza and subsequently failed to protect against influenza as effectively as CCR4-sufficient, lung DC–activated T cells. There was a rise in the expression of CCR4 ligands in the lungs of infected mice, which peaked at 4 d after infection and correlated with the trafficking defect of lung DC–activated, CCR4-deficient T cells. The detrimental impact of this early trafficking defect is in agreement with a study demonstrating that survival is compromised the most when antigen-specific T cells are eliminated early in the course of infection with influenza (Hamada et al., 2013). The deleterious impact of CCR4 deficiency in the ability of lung DC–activated T cells to protect against influenza could perhaps be explained by the observation that influenza-specific CD4$^+$ T cells contribute to viral clearance by inducing the early release of a large number of innate inflammatory cytokines and chemokines within 40 h of infection (Strutt et al., 2010). Our observation with regard to influenza is consistent with the literature that supports a role for CCR4 in T cell immune responses to other respiratory pathogens (Freeman et al., 2006; Hartl et al., 2006; Stolberg et al., 2011; Shankar et al., 2012). We observed that recipients of CCR4-deficient, lung DC–activated T cells lost more weight (23 vs. 19%) for longer (8 vs. 7 d), had lower rate of survival (70 vs. 90%), and continued to harbor the influenza virus at day 10 after infection. Therefore, our data collectively demonstrate that lung DCs imprint T cell lung homing in part through CCR4.

Our study illuminates the role of DCs in CCR4 expression and the role of CCR4 in tissue-selective T cell homing. Although nearly all CLA$^+$CD4$^+$ T cells in the skin and the blood are CCR4$^+$ (Campbell et al., 1999; Kunkel et al., 2002; Soler et al., 2003; Clark et al., 2006), skin DCs have not been shown to imprint CCR4 expression. Instead, skin DCs imprint CCR10, which is expressed only by a small subset of skin homing T cells (Sigmundsdottir et al., 2007). Recently, epidermal keratinocyte have been shown to imprint CCR8 (McCully et al., 2012) and not CCR4. Furthermore, although nearly all memory CLA$^+$ T cells in the blood are CCR4$^+$, not all peripheral blood CCR4$^+$ T cells are CLA$^+$ (Soler et al., 2003). This observation indicates that despite its prominent role in T cell trafficking into the skin (Reiss et al., 2001; Campbell et al., 2007; Oyoshi et al., 2011), CCR4 is not an exclusive skin-homing molecule. In addition to dermal post capillary venules (Campbell et al., 1999), lung epithelial (Kawasaki et al., 2001) and endothelial cells express CCL17, a CCR4 ligand. CCR4 contributes to effector and regulatory T cell trafficking into the lung during inflammation (Lloyd et al., 2000; Mikhak et al., 2009; Afshar et al., 2013), and CCR4 deficiency in regulatory T cells results in severe inflammatory disease not only in the skin but also in the lung (Sather et al., 2007). Our data demonstrate that lung DCs imprint the expression of CCR4 on T cells and that CCR4 expression by lung DC–activated T cells promotes T cell trafficking into the lung at homeostasis as well as in response to inhaled antigens and the pulmonary pathogen influenza.

We saw no statistically significant difference in the expression of CCR4, $\alpha 4 \beta 7$, and E-selectin ligand between in vitro–generated lung DC– and SLN DC–activated T cells after 5 d in culture. The many similarities in the expression of trafficking molecules between lung and SLN DC–activated T cells and the expression of CCR4 ligands in both the lung (Kawasaki et al., 2001) and the skin (Campbell et al., 1999; Chong et al., 2004) suggest that SLN DC–activated T cells could potentially home to the lung and lung DC–activated T cells could potentially home to the skin. Consistent with this lung–skin connection, small pox vaccination via skin scarification has been shown to generate lung-resident memory T cells that provide partial protection against fatal small pox pulmonary infection (Liu et al., 2010). However, we observed that despite their in vitro similarities in the expression of trafficking molecules, lung and SLN DC–activated T cells trafficked differentially in vivo. The smallest differential was observed within 4 h of adoptive transfer in the absence of antigen, when lung DC–activated T cells demonstrated a 1.5-fold homing advantage into the lung and a 1.4-fold homing advantage into PPs compared with SLN DC–activated T cells. The in vivo trafficking differential between lung and SLN DC–activated T cells widened with antigen exposure over time. Lung DC–activated T cells trafficked 2.3- to 6.6-fold more efficiently into the lung compared with SLN DC–activated T cells in response to inhaled antigen challenges or pulmonary infection with influenza. Furthermore, SLN DC–activated T cells trafficked 2.5-fold more efficiently into the ear skin

compared with lung DC–activated T cells in response to tape stripping and epicutaneous antigen challenges. These data collectively suggest that the expression of trafficking molecules on lung and SLN DC–activated T cells might diverge in vivo upon antigen exposure.

We show that lung DC imprinting leads to both tissue-selective and systemic T cell distribution. Lung DCs endow T cells with a lung-homing advantage and also license them for entry into other epithelial organs at homeostasis. Lung DC–activated T cells home into PPs as well as MLN DC–activated T cells and home into SLNs better than MLN DC–activated T cells. Furthermore, lung DC–activated T cells home into SLNs as well as SLN DC–activated T cells and home into PPs better than SLN DC–activated T cells. Therefore, lung DC–activated T cells are more liberal in their systemic distribution compared with SLN and MLN DC–activated T cells. The wide distribution of lung DC–activated T cells could be explained by their expression of $\alpha4\beta7$ and E-selectin ligand. Lung DC imprinting appears compatible with the acquisition of systemic T cell immunity. In systemic T cell immunity, exposure to a pathogen in one tissue leads to distribution of pathogen-experienced T cells both into the original site and into other tissues, where some pathogen-specific T cells persist long-term (Masopust et al., 2001, 2004), and provide a ready line of T cell defense for swift eradication of invading pathogens through immediate cytokine release and cytotoxic activities (Masopust et al., 2001; Teijaro et al., 2011; Jiang et al., 2012). Our findings imply that exposure to inhaled antigen results in the generation of antigen-experienced T cells that not only populate the lung but also could contribute to the pool of tissue-resident T cells in other epithelial organs at distant sites. Indeed, influenza-specific memory T cells are detected in small intestinal epithelium after intranasal influenza infection (Masopust et al., 2010). Furthermore, antigen-specific T cells activated in lung-draining LNs are found in nondraining SLNs and MLNs within 5 d after intranasal exposure (Ciabattini et al., 2011). Collectively, our results imply that inhalational delivery of vaccines might provide better lung immunity while also establishing efficient T cell protection at other epithelial organs.

Our data suggest that lung-imprinting DCs reside in the lung and not in lung-draining LNs at homeostasis. One possible explanation is that lung-imprinting DCs are not present in the TLN in sufficient numbers at baseline to imprint T cell lung homing. Another possibility is that a factor in the TLN inhibits the function of lung-imprinting DCs at homeostasis (Lee et al., 2009). However, we observed that TLN DCs acquired the ability to imprint T cell lung homing 24 h, but not 30 min, after inhaled antigen exposure, when there is sufficient time for DC migration from the lung to the TLN (Vermaelen et al., 2001). This suggests that lung-imprinting DCs are migratory DCs that travel from the lung to the TLN upon exposure to inhaled antigen and take with them the ability to imprint lung homing to the TLN. It also suggests that passive drainage of antigen or soluble factors from the lung to the TLN, which occurs within minutes (Gretz et al., 2000), is not sufficient to endow TLN DCs with lung-imprinting abilities. The number of lung-imprinting DCs that migrate from the lung to the TLN in response to inhaled antigen must make up a small fraction of all lung-imprinting DCs in the lung as the ability of lung DCs to imprint lung homing did not change with inhaled antigen exposure. Our observations collectively suggest that T cells activated in the TLN, perhaps in response to circulating antigens, are not imprinted with lung homing, a phenomenon which might prevent excessive T cell–mediated immune responses in the lung. T cell lung imprinting in the TLN requires inhaled antigen exposure and mobilization of lung-imprinting DCs from the lung to the TLN.

Our findings advance our understanding of tissue-selective T cell imprinting at epithelial surfaces. We show that lung DCs imprint T cell lung homing and, in doing so, promote lung immunity against pulmonary infection with influenza in part via CCR4. Our findings suggest that inhalational delivery of a vaccine against influenza might improve protection against this important global human pathogen. Our study opens up a large area of research to fully define the mechanisms through which DC lung imprinting is accomplished. Future studies will define the role of lung DC subsets and lung microenvironmental factors and the nature of DC–T cell interactions in T cell lung imprinting.

MATERIALS AND METHODS

Mice. All mice were in the C57BL/6 background. Wild-type Thy1.2$^+$ male C57BL/6 mice were purchased from the National Cancer Institute, Taconic, or the Jackson Laboratory and used as DC donors or recipients in adoptive transfer experiments. Thy1.1$^+$ OTII mice, which are transgenic for the TCR recognizing pOVA$_{323–339}$, were a gift from P. Shrikant (Roswell Park Cancer Institute, Buffalo, NY), bred in our laboratory, and used as CD4$^+$ T cell donors. In some experiments, Thy1.2$^+$ OTII mice were purchased from the Jackson Laboratory and were used as CD4$^+$ T cell donors, and Thy1.1$^+$ mice, also from the Jackson Laboratory, were used as recipients. Thy1.2$^+$CCR4$^{-/-}$ OTII mice, also used as CD4$^+$ T cell donors, were backcrossed at least 10 generations to C57BL/6, generated as previously described, and bred in our laboratory (Chvatchko et al., 2000; Mikhak et al., 2009). In experiments comparing OTII and CCR4$^{-/-}$ OTII cells, Thy1.2$^+$ OTII cells that had been purchased from the Jackson Laboratory and bred in our animal facility were used. Thy1.2$^+$ OTI mice, which are transgenic for the TCR recognizing pOVA$_{257–264}$, were purchased from the Jackson Laboratory. As a control for mice housed solely in our animal facility, we repeated our experiments using mice housed in different animal facilities. Similar results were obtained when we used Thy1.1$^+$ OTII mice bred in our animal facility or Thy1.2$^+$ OTII mice bred at the Jackson Laboratory as T cell donors and whether we used naive Thy1.2$^+$ or Thy1.1$^+$ C57BL/6 mice from the National Cancer Institute, Taconic Farms, or Jackson Laboratory as recipients. Mice were age and gender matched and used at 6–8 wk of age. Mice were housed under specific pathogen–free conditions. All experiments were performed according to protocols approved by the Massachusetts General Hospital Subcommittee on Research Animal Care.

In vivo expansion of DCs, DC isolation, and DC–T cell cultures. A minimum of 1 million DCs from each site was needed for DC–T cell cultures to generate enough T cells to inject three to four mice per group per experiment. To expand DC numbers, naive C57BL/6 mice were injected in the interscapular area with B16 Flt3L-secreting melanoma cells, a gift from G. Dranoff (Dana-Farber Cancer Institute, Boston, MA; Mach et al., 2000). On days 12–14, PBS-flushed lungs, TLN, spleen, SLN, MLN, ears (for DC

isolation from the skin), jejunum, and ileum (for DC isolation from LP) were isolated from the same donor pool. Minced lungs, spleens, and LNs were digested in RPMI medium containing 0.52 Wunsch U/ml of Liberase and 60 U/ml DNase I (both from Roche) at 37°C. Length of digestion was optimized for each tissue to maximize yield and minimize cell death. Red blood cell lysis buffer (Sigma-Aldrich) was used for 1–3 min when needed. LP and skin DCs were isolated as described previously (Jakubzick et al., 2008; Helft and Merad, 2010). CD11c⁺ cells were isolated using anti-CD11c microbeads (Miltenyi Biotec). In some experiments, Flt3L-expanded mice were given an intranasal dose of OVA (50 µl at 2 mg/ml; Sigma-Aldrich) with or without 8 µg of intranasal CCR4 or CCR7 blocking antibody (both from Capralogics; Fainaru et al., 2005), and CD11c⁺ cells were isolated from the lung and TLN either 30 min or 24 h later. In control experiments, Flt3L-expanded mice were given an intranasal dose of FITC-labeled OVA (50 µl at 2 mg/ml; Molecular Probes) with or without intranasal CCR4 or CCR7 blocking antibody as above, and TLNs were harvested 48 h later. In other experiments, adequate numbers of lung, spleen, and SLN CD11c⁺ cells were obtained by using up to 20 naive unexpanded C57BL/6 mice and pooling each tissue. In those experiments, single cell preparations of unexpanded tissues were rested overnight before isolation of CD11c⁺ cells. CD4⁺ T cells were isolated from the pooled LNs and spleen of OTII mice (Thy1.1⁺ or Thy1.2⁺ OTII or Thy1.2⁺CCR4⁻/⁻ OTII depending on the experiment) using Dynabeads (Invitrogen). DC–T cell cultures were established at a 1:1 ratio using pOVA$_{323–339}$ (final concentration = 2 µg/ml or 1.1 µM; Peptides International), without exogenous cytokines in complete culture medium (RPMI supplemented with 10% heat-inactivated fetal calf serum, 10 mM Hepes, 2 mM L-glutamine, 50 µM β-mercaptoethanol, 100 U/ml penicillin, 100 µg/ml streptomycin, and 0.1 mM nonessential amino acids) at 1 million cells per ml in flat bottom 96-well plates. Cells were fed with fresh media (not containing any cytokines) daily starting on day 2 of culture and split 1:2 starting on day 3. On day 5 of culture, surface staining was performed for trafficking molecules. On day 6 of culture, surface staining for activation markers and intracellular staining for cytokines were performed as described previously (Mikhak et al., 2006) to ensure equal differentiation and activation among groups.

CD8⁺ T cells were isolated from the pooled LNs and spleen of OTI mice via negative selection using the mouse CD8a⁺ T cell isolation kit II from Miltenyi Biotec. DCs were pulsed with pOVA$_{257–264}$ (final concentration = 9.6 µg/ml or 10 µM; Peptides International) at 10 million cells per ml for 1 h and washed twice. DC–T cell cultures were established at a 1:2 ratio without exogenous cytokines in complete culture media at 1.5 million cells per ml in flat bottom 96-well plates. Cells were fed and split as above.

In vivo separate adoptive transfer model. On day 6 or 7, DC-activated T cells were adoptively transferred via the tail vein, at 2×10^6 cells in 0.5 ml per mouse, into separate naive recipient mice. Thy1.1⁺ OTII cells were transferred into Thy1.2⁺ recipient mice. Thy1.2⁺ OTII or OTI cells were transferred into Thy1.1⁺ recipients. 24–72 h after adoptive transfer, mice were given three daily aerosolized 5% OVA (Sigma-Aldrich) challenges, for 20 min each day, using a nebulizer (Pulmo Aide). In some experiments, mice were evaluated 72 h after adoptive transfer without any OVA challenges. In other experiments, mice were given one oral or one i.p. challenge with 100 µl of 5% OVA. For in vivo proliferation experiments, mice were injected with 0.2 ml BrdU (Sigma-Aldrich) i.p. at 10 mg/ml before the third OVA challenge. 2 h after the third challenge, TLNs were isolated and the percentage of BrdU⁺CD4⁺Thy1.1⁺ cells in the lymphocyte gate was determined. In other experiments, in vitro–generated CD4⁺ T cells were resuspended at 4×10^5 cells/ml on day 5, treated with PTX (100 ng/ml; Sigma-Aldrich) or vehicle (distilled H$_2$O) for 24 h, and then washed twice with PBS before their adoptive transfer. To assess T cell trafficking into the ear skin, DC-activated Thy1.2⁺ OTII cells were adoptively transferred via the tail vein, at 12×10^6 cells in 0.5 ml per mouse, into separate Thy1.1⁺ recipient mice. 24 h after adoptive transfer, the outer surface of each ear was tape stripped 12 times using Scotch Matte Finish Magic Tape (3M), and 25 µl of 5% OVA was applied epicutaneously. The procedure was repeated daily for 3 d.

In vivo competitive adoptive transfer model. On day 6, lung DC–activated T cells were labeled with 1 mM CFSE (Molecular Probes), whereas MLN and SLN DC–activated T cells were labeled separately with 9 mM CMTMR (Molecular Probes) for 15 min at 37°C, spun over fetal calf serum, incubated in RPMI at 37°C for 15 min, and washed in PBS twice. CFSE-labeled, lung DC–activated T cells were mixed with CMTMR-labeled, MLN or SLN DC–activated T cells at 1:1 ratio at 20 million cells per ml and injected via the tail vein into naive recipient mice at 0.5 ml per mouse. The ratio of input cells was determined using flow cytometry before adoptive transfer. 4 h after adoptive transfer, the lung, spleen, PPs, and SLNs (inguinal) were isolated. Single cell suspensions from each site were prepared and stained with 7-AAD and allophycocyanin (APC)-labeled, anti–mouse CD4 antibody. The percentage of CFSE-labeled (lung DC activated) and CMTMR-labeled (MLN or SLN DC activated) cells in the 7-AAD⁻CD4⁺ gate within the lymphocyte gate was determined in each tissue by flow cytometry. HI was calculated as [percentage of CFSE⁺ cells/percentage of CMTMR⁺ cells]$_{tissue}$/[percentage of CFSE⁺ cells/percentage of CMTMR⁺ cells]$_{input}$. In control experiments, dyes were switched with similar results.

Recovery of mouse tissue leukocytes. BAL was performed 24 h after the final aerosol challenge with six 0.5-ml aliquots of PBS with 0.6 mM EDTA. PBS-flushed lungs were minced and digested for 30 min as above. Single cell suspensions were made from lungs, spleen, PPs, and SLNs after passage through a 70-µm cell strainer (Thermo Fisher Scientific). Red blood cells were lysed as above when needed. To recover T cells from the mouse ear, ears were minced for 1 min, digested in 8 ml HBSS containing 10% fetal calf serum and Collagenase IV (Sigma-Aldrich) at 154 U/ml at 37°C for 45 min, and passed through a 70-µm cell strainer. Isolation of lymphocytes from LP was performed as previously described (Shang et al., 2009). Live cells were counted with a hemocytometer. To determine the number of adoptively transferred cells in each compartment, the total number of cells was multiplied by the percentage of CD4⁺Thy1.1⁺ cells when Thy1.1⁺ OTII cells were transferred into Thy1.2⁺ recipients or by the percentage of CD4⁺Thy1.2⁺ cells when Thy1.2⁺ OTII cells were transferred into Thy1.1⁺ recipients.

Infection with influenza. 3 d after adoptive transfer of DC-activated T cells, recipient mice were anesthetized with i.p. injection of 80–100 mg/kg ketamine HCl and 12 mg/kg xylazine. Mice were infected with a live OVA$_{323–339}$-expressing PR8-H1N1 influenza virus (Thomas et al., 2006) at 10^5 PFU in 50 µl PBS per mouse intranasally. Some mice were euthanized on day 3 after infection, and the lungs were harvested and the number of adoptively transferred T cells was determined as described above. Other mice were monitored for weight loss and survival daily for 14–18 d.

Flow cytometry. Flow cytometry was performed on a FACScan (BD) cytofluorometer, and results were analyzed with FlowJo software (Tree Star). Cells were incubated with anti-FcγIII/FcγII receptor (BioLegend) for 10 min and then stained with fluorescent-labeled monoclonal antibodies from R&D Systems (CCR1-3, CCR9-10, CXCR2, and CXCR5-6), eBioscience (CCR5, CXCR4, CD29, CD49e, CD103, CD43, and CD41), BioLegend (CD4, CD11c, CD44, Thy1.1, Thy1.2, IL-4, IL-17a, IFN-γ, CD103, CCR4, CCR6, CCR7, CXCR3, CD61, b7, CD104, CD49a, CD49b, CD49f, CD51, CD11b, CD43, MHC II, CD86, CD2, and F4/80), and BD (α4β7, CD3, CD19, CD69, CD25, CD62L, CD49a, VLA-4, and LFA-1). Recombinant mouse E-selectin/CD62E Fc chimera (R&D Systems) and APC-conjugated affinity pure F(ab′)2 fragment goat anti–human IgG Fcγ fragment specific (Jackson ImmunoResearch Laboratories, Inc.) were used for E-selectin ligand staining. For proliferation and apoptosis, APC BrdU flow kit (BD) and 7-AAD Viability Staining Solution (BioLegend) were used, respectively. Staining for CCR8 was not performed because of a lack of commercially available validated antibodies.

In vitro–generated, DC-activated T cells were rested (by replacing the media in each well with fresh media) for 4 h at 37°C before staining for trafficking molecules. All staining was performed for 20 min at 4°C except for CCR7 staining, which was performed for 30 min at 37°C. Freshly prepared, azide-free FACS buffer was used.

PBS-flushed, naive mouse whole lungs were minced and digested in 5 ml RPMI medium plus Liberase and DNase I as above for 30 min at 37°C. Single cell suspensions (2 million cells per ml) were rested for 3–4 h at 37°C before staining for chemokine receptors. In control experiments, we confirmed that digestion with the above protocol did not affect CCR4, CCR6, CCR5, CD103, CXCR2, CXCR4, CD11b, CD41, and CD49a epitopes.

QPCR. Total RNA was isolated from naive mouse lungs using RNeasy (QIAGEN). RNA was converted to cDNA and analyzed by QPCR as previously described (Mikhak et al., 2006) using the Mx4000TM Multiplex Quantitative PCR System (Agilent Technologies). Viral RNA copies for the polymerase gene of the PR8 influenza virus were determined using the following primers: forward primer, 5′-CGGTCCAAATTCCTGCTGA-3′; and reverse primer, 5′-CATTGGGTTCCTTCCATCCA-3′ (Cho et al., 2012). Chemokine RNA copies were determined using the following primers: CXCL9 forward primer, 5′-AATGCACGATGCTCCTGCA-3′; and reverse primer, 5′-AGGTCTTTGAGGGATTTGTAGTGG-3′; CXCL10 forward primer, 5′-GCCGTCATTTTCTGCCTCA-3′; and reverse primer, 5′-CGTCCTTGCGAGAGGGATC-3′; CCL17 forward primer, 5′-CAGGGATGCCATCGTGTTTC-3′; and reverse primer, 5′-CACCA-ATCTGATGGCCTTCTT-3′; CCL20 forward primer, 5′-TGGGTA-CTGCTGGCTCACCT-3′; and reverse primer, 5′-CGAGAGGCAACAG-TCGTAGTTG-3′; and CCL22 forward primer, 5′-TACATCCGTCACC-CTCTGCC-3′; and reverse primer, 5′-CGGTTATCAAAACAACGCCAG-3′.

Histology. Lungs were flushed with PBS and maximally inflated with 10% formalin. Multiple paraffin-embedded 5-mm sections were prepared and stained with hematoxylin and eosin (H&E). A blinded investigator scored the extent of cellular infiltration based on 0 = normal, 1 = some cells, 2 = a single layer, 3 = two to three layers, and 4 = four or more layers of cells around airways and blood vessels. For each slide, the mean of 21 airways and 24 blood vessels were scored and used to calculate a mean histopathologic score.

Immunohistochemistry. Paraffin-embedded slides were treated with xylene (twice, 5 min), 100% ethanol (twice, 2 min), 90%, 80%, and 75% ethanol (once, 2 min), water, and PBS. After antigen retrieval with Antigen Decloaker (Biocare Medical), slides were rinsed with PBS and blocked with Sniper Block (Biocare Medical) for 10 min. Slides were treated with human/mouse CCL17 (TARC) antibody (at 1:50 dilution) or control goat anti–human Ig (both from Santa Cruz Biotechnology, Inc.) overnight at 4°C, washed three times in PBS, incubated for 35 min with biotinylated anti–goat antibody (Vector Laboratories), and washed three times with PBS. Protein expression was visualized using streptavidin-peroxidase and DAB Plus Substrate System (DAKO). Slides were counterstained with hematoxylin (Olkhanud et al., 2009).

Statistical analysis. Experiments were performed at least twice with a minimum of three mice per group per experiment. Each mouse was used as a data point. Cumulative data are presented as mean ± SEM. Statistical significance was determined using the Student's two-tailed t test in experiments comparing two groups. ANOVA was used in experiments comparing more than two groups. Survival curves were plotted and analyzed by Prism 5.0 software (GraphPad Software). $P < 0.05$ was considered significant, and *, $P < 0.05$; **, $P < 0.005$; ***, $P < 0.0005$; and ****, $P < 0.00005$ are used throughout.

REFERENCES

Afshar, R., J.P. Strassner, E. Seung, B. Causton, J.L. Cho, R.S. Harris, D.L. Hamilos, B.D. Medoff, and A.D. Luster. 2013. Compartmentalized chemokine-dependent regulatory T-cell inhibition of allergic pulmonary inflammation. *J. Allergy Clin. Immunol.* 131:1644–1652. http://dx.doi.org/10.1016/j.jaci.2013.03.002

Campbell, D.J., and E.C. Butcher. 2002. Rapid acquisition of tissue-specific homing phenotypes by CD4+ T cells activated in cutaneous or mucosal lymphoid tissues. *J. Exp. Med.* 195:135–141. http://dx.doi.org/10.1084/jem.20011502

Campbell, J.J., G. Haraldsen, J. Pan, J. Rottman, S. Qin, P. Ponath, D.P. Andrew, R. Warnke, N. Ruffing, N. Kassam, et al. 1999. The chemokine receptor CCR4 in vascular recognition by cutaneous but not intestinal memory T cells. *Nature.* 400:776–780. http://dx.doi.org/10.1038/23495

Campbell, J.J., D.J. O'Connell, and M.A. Wurbel. 2007. Cutting Edge: Chemokine receptor CCR4 is necessary for antigen-driven cutaneous accumulation of CD4 T cells under physiological conditions. *J. Immunol.* 178:3358–3362.

Centers for Disease Control and Prevention (CDC). 2013. Interim adjusted estimates of seasonal influenza vaccine effectiveness - United States, February 2013. *MMWR Morb. Mortal. Wkly. Rep.* 62:119–123. http://www.cdc.gov/mmwr/preview/mmwrhtml/mm6207a2.htm

Cho, J.L., M.I. Roche, B. Sandall, A.L. Brass, B. Seed, R.J. Xavier, and B.D. Medoff. 2012. Enhanced Tim3 activity improves survival after influenza infection. *J. Immunol.* 189:2879–2889. http://dx.doi.org/10.4049/jimmunol.1102483

Chong, B.F., J.E. Murphy, T.S. Kupper, and R.C. Fuhlbrigge. 2004. E-selectin, thymus- and activation-regulated chemokine/CCL17, and intercellular adhesion molecule-1 are constitutively coexpressed in dermal microvessels: a foundation for a cutaneous immunosurveillance system. *J. Immunol.* 172:1575–1581.

Chvatchko, Y., A.J. Hoogewerf, A. Meyer, S. Alouani, P. Juillard, R. Buser, F. Conquet, A.E. Proudfoot, T.N. Wells, and C.A. Power. 2000. A key role for CC chemokine receptor 4 in lipopolysaccharide-induced endotoxic shock. *J. Exp. Med.* 191:1755–1764. http://dx.doi.org/10.1084/jem.191.10.1755

Ciabattini, A., E. Pettini, F. Fiorino, G. Prota, G. Pozzi, and D. Medaglini. 2011. Distribution of primed T cells and antigen-loaded antigen presenting cells following intranasal immunization in mice. *PLoS ONE.* 6:e19346. http://dx.doi.org/10.1371/journal.pone.0019346

Clark, R.A., B. Chong, N. Mirchandani, N.K. Brinster, K. Yamanaka, R.K. Dowgiert, and T.S. Kupper. 2006. The vast majority of CLA+ T cells are resident in normal skin. *J. Immunol.* 176:4431–4439.

Dudda, J.C., J.C. Simon, and S. Martin. 2004. Dendritic cell immunization route determines CD8+ T cell trafficking to inflamed skin: role for tissue microenvironment and dendritic cells in establishment of T cell-homing subsets. *J. Immunol.* 172:857–863.

Fainaru, O., D. Shseyov, S. Hantisteanu, and Y. Groner. 2005. Accelerated chemokine receptor 7-mediated dendritic cell migration in Runx3 knockout mice and the spontaneous development of asthma-like disease. *Proc. Natl. Acad. Sci. USA.* 102:10598–10603. http://dx.doi.org/10.1073/pnas.0504787102

Freeman, C.M., V.R. Stolberg, B.C. Chiu, N.W. Lukacs, S.L. Kunkel, and S.W. Chensue. 2006. CCR4 participation in Th type 1 (mycobacterial) and Th type 2 (schistosomal) anamnestic pulmonary granulomatous responses. *J. Immunol.* 177:4149–4158.

Gretz, J.E., C.C. Norbury, A.O. Anderson, A.E. Proudfoot, and S. Shaw. 2000. Lymph-borne chemokines and other low molecular weight molecules reach high endothelial venules via specialized conduits while

a functional barrier limits access to the lymphocyte microenvironments in lymph node cortex. *J. Exp. Med.* 192:1425–1440. http://dx.doi.org/10.1084/jem.192.10.1425

Hamada, H., E. Bassity, A. Flies, T.M. Strutt, Mde.L. Garcia-Hernandez, K.K. McKinstry, T. Zou, S.L. Swain, and R.W. Dutton. 2013. Multiple redundant effector mechanisms of CD8+ T cells protect against influenza infection. *J. Immunol.* 190:296–306. http://dx.doi.org/10.4049/jimmunol.1200571

Hao, X., T.S. Kim, and T.J. Braciale. 2008. Differential response of respiratory dendritic cell subsets to influenza virus infection. *J. Virol.* 82:4908–4919. http://dx.doi.org/10.1128/JVI.02367-07

Hartl, D., M. Griese, M. Kappler, G. Zissel, D. Reinhardt, C. Rebhan, D.J. Schendel, and S. Krauss-Etschmann. 2006. Pulmonary T(H)2 response in *Pseudomonas aeruginosa*-infected patients with cystic fibrosis. *J. Allergy Clin. Immunol.* 117:204–211. http://dx.doi.org/10.1016/j.jaci.2005.09.023

Helft, J., and M. Merad. 2010. Isolation of cutaneous dendritic cells. *Methods Mol. Biol.* 595:231–233. http://dx.doi.org/10.1007/978-1-60761-421-0_15

Hoft, D.F., E. Babusis, S. Worku, C.T. Spencer, K. Lottenbach, S.M. Truscott, G. Abate, I.G. Sakala, K.M. Edwards, C.B. Creech, et al. 2011. Live and inactivated influenza vaccines induce similar humoral responses, but only live vaccines induce diverse T-cell responses in young children. *J. Infect. Dis.* 204:845–853. http://dx.doi.org/10.1093/infdis/jir436

Iwata, M., A. Hirakiyama, Y. Eshima, H. Kagechika, C. Kato, and S.Y. Song. 2004. Retinoic acid imprints gut-homing specificity on T cells. *Immunity*. 21:527–538. http://dx.doi.org/10.1016/j.immuni.2004.08.011

Jakubzick, C., M. Bogunovic, A.J. Bonito, E.L. Kuan, M. Merad, and G.J. Randolph. 2008. Lymph-migrating, tissue-derived dendritic cells are minor constituents within steady-state lymph nodes. *J. Exp. Med.* 205:2839–2850. http://dx.doi.org/10.1084/jem.20081430

Jiang, X., R.A. Clark, L. Liu, A.J. Wagers, R.C. Fuhlbrigge, and T.S. Kupper. 2012. Skin infection generates non-migratory memory CD8+ T(RM) cells providing global skin immunity. *Nature*. 483:227–231. http://dx.doi.org/10.1038/nature10851

Johansson-Lindbom, B., M. Svensson, M.A. Wurbel, B. Malissen, G. Márquez, and W. Agace. 2003. Selective generation of gut tropic T cells in gut-associated lymphoid tissue (GALT): requirement for GALT dendritic cells and adjuvant. *J. Exp. Med.* 198:963–969. http://dx.doi.org/10.1084/jem.20031244

Kallinich, T., S. Schmidt, E. Hamelmann, A. Fischer, S. Qin, W. Luttmann, J.C. Virchow, and R.A. Kroczek. 2005. Chemokine-receptor expression on T cells in lung compartments of challenged asthmatic patients. *Clin. Exp. Allergy*. 35:26–33. http://dx.doi.org/10.1111/j.1365-2222.2004.02132.x

Kawasaki, S., H. Takizawa, H. Yoneyama, T. Nakayama, R. Fujisawa, M. Izumizaki, T. Imai, O. Yoshie, I. Homma, K. Yamamoto, and K. Matsushima. 2001. Intervention of thymus and activation-regulated chemokine attenuates the development of allergic airway inflammation and hyper-responsiveness in mice. *J. Immunol.* 166:2055–2062.

Koelle, D.M., Z. Liu, C.M. McClurkan, M.S. Topp, S.R. Riddell, E.G. Pamer, A.S. Johnson, A. Wald, and L. Corey. 2002. Expression of cutaneous lymphocyte-associated antigen by CD8(+) T cells specific for a skin-tropic virus. *J. Clin. Invest.* 110:537–548.

Kunkel, E.J., J. Boisvert, K. Murphy, M.A. Vierra, M.C. Genovese, A.J. Wardlaw, H.B. Greenberg, M.R. Hodge, L. Wu, E.C. Butcher, and J.J. Campbell. 2002. Expression of the chemokine receptors CCR4, CCR5, and CXCR3 by human tissue-infiltrating lymphocytes. *Am. J. Pathol.* 160:347–355. http://dx.doi.org/10.1016/S0002-9440(10)64378-7

Lambrecht, B.N., and H. Hammad. 2012. Lung dendritic cells in respiratory viral infection and asthma: from protection to immunopathology. *Annu. Rev. Immunol.* 30:243–270. http://dx.doi.org/10.1146/annurev-immunol-020711-075021

Lee, H.K., M. Zamora, M.M. Linehan, N. Iijima, D. Gonzalez, A. Haberman, and A. Iwasaki. 2009. Differential roles of migratory and resident DCs in T cell priming after mucosal or skin HSV-1 infection. *J. Exp. Med.* 206:359–370. http://dx.doi.org/10.1084/jem.20080601

Liu, L., R.C. Fuhlbrigge, K. Karibian, T. Tian, and T.S. Kupper. 2006. Dynamic programming of CD8+ T cell trafficking after live viral immunization. *Immunity*. 25:511–520. http://dx.doi.org/10.1016/j.immuni.2006.06.019

Liu, L., Q. Zhong, T. Tian, K. Dubin, S.K. Athale, and T.S. Kupper. 2010. Epidermal injury and infection during poxvirus immunization is crucial for the generation of highly protective T cell–mediated immunity. *Nat. Med.* 16:224–227. http://dx.doi.org/10.1038/nm.2078

Lloyd, C.M., T. Delaney, T. Nguyen, J. Tian, C. Martinez-A, A.J. Coyle, and J.C. Gutierrez-Ramos. 2000. CC chemokine receptor (CCR)3/eotaxin is followed by CCR4/monocyte-derived chemokine in mediating pulmonary T helper lymphocyte type 2 recruitment after serial antigen challenge in vivo. *J. Exp. Med.* 191:265–274. http://dx.doi.org/10.1084/jem.191.2.265

Mach, N., S. Gillessen, S.B. Wilson, C. Sheehan, M. Mihm, and G. Dranoff. 2000. Differences in dendritic cells stimulated in vivo by tumors engineered to secrete granulocyte-macrophage colony-stimulating factor or Flt3-ligand. *Cancer Res.* 60:3239–3246.

Masopust, D., V. Vezys, A.L. Marzo, and L. Lefrançois. 2001. Preferential localization of effector memory cells in nonlymphoid tissue. *Science*. 291:2413–2417. http://dx.doi.org/10.1126/science.1058867

Masopust, D., V. Vezys, E.J. Usherwood, L.S. Cauley, S. Olson, A.L. Marzo, R.L. Ward, D.L. Woodland, and L. Lefrançois. 2004. Activated primary and memory CD8 T cells migrate to nonlymphoid tissues regardless of site of activation or tissue of origin. *J. Immunol.* 172:4875–4882.

Masopust, D., D. Choo, V. Vezys, E.J. Wherry, J. Duraiswamy, R. Akondy, J. Wang, K.A. Casey, D.L. Barber, K.S. Kawamura, et al. 2010. Dynamic T cell migration program provides resident memory within intestinal epithelium. *J. Exp. Med.* 207:553–564. http://dx.doi.org/10.1084/jem.20090858

McCully, M.L., K. Ladell, S. Hakobyan, R.E. Mansel, D.A. Price, and B. Moser. 2012. Epidermis instructs skin homing receptor expression in human T cells. *Blood*. 120:4591–4598. http://dx.doi.org/10.1182/blood-2012-05-433037

Mikhak, Z., C.M. Fleming, B.D. Medoff, S.Y. Thomas, A.M. Tager, G.S. Campanella, and A.D. Luster. 2006. STAT1 in peripheral tissue differentially regulates homing of antigen-specific Th1 and Th2 cells. *J. Immunol.* 176:4959–4967.

Mikhak, Z., M. Fukui, A. Farsidjani, B.D. Medoff, A.M. Tager, and A.D. Luster. 2009. Contribution of CCR4 and CCR8 to antigen-specific T(H)2 cell trafficking in allergic pulmonary inflammation. *J. Allergy Clin. Immunol.* 123:67–73. http://dx.doi.org/10.1016/j.jaci.2008.09.049

Mora, J.R., M.R. Bono, N. Manjunath, W. Weninger, L.L. Cavanagh, M. Rosemblatt, and U.H. Von Andrian. 2003. Selective imprinting of gut-homing T cells by Peyer's patch dendritic cells. *Nature*. 424:88–93. http://dx.doi.org/10.1038/nature01726

Mora, J.R., G. Cheng, D. Picarella, M. Briskin, N. Buchanan, and U.H. von Andrian. 2005. Reciprocal and dynamic control of CD8 T cell homing by dendritic cells from skin- and gut-associated lymphoid tissues. *J. Exp. Med.* 201:303–316. http://dx.doi.org/10.1084/jem.20041645

Olkhanud, P.B., D. Baatar, M. Bodogai, F. Hakim, R. Gress, R.L. Anderson, J. Deng, M. Xu, S. Briest, and A. Biragyn. 2009. Breast cancer lung metastasis requires expression of chemokine receptor CCR4 and regulatory T cells. *Cancer Res.* 69:5996–6004. http://dx.doi.org/10.1158/0008-5472.CAN-08-4619

Osterholm, M.T., N.S. Kelley, A. Sommer, and E.A. Belongia. 2012. Efficacy and effectiveness of influenza vaccines: a systematic review and meta-analysis. *Lancet Infect. Dis.* 12:36–44. http://dx.doi.org/10.1016/S1473-3099(11)70295-X

Oyoshi, M.K., A. Elkhal, J.E. Scott, M.A. Wurbel, J.L. Hornick, J.J. Campbell, and R.S. Geha. 2011. Epicutaneous challenge of orally immunized mice redirects antigen-specific gut-homing T cells to the skin. *J. Clin. Invest.* 121:2210–2220. http://dx.doi.org/10.1172/JCI43586

Purwar, R., J. Campbell, G. Murphy, W.G. Richards, R.A. Clark, and T.S. Kupper. 2011. Resident memory T cells (T(RM)) are abundant in human lung: diversity, function, and antigen specificity. *PLoS ONE*. 6:e16245. http://dx.doi.org/10.1371/journal.pone.0016245

Reinhardt, R.L., S.J. Kang, H.E. Liang, and R.M. Locksley. 2006. T helper cell effector fates—who, how and where? *Curr. Opin. Immunol.* 18:271–277. http://dx.doi.org/10.1016/j.coi.2006.03.003

Reiss, Y., A.E. Proudfoot, C.A. Power, J.J. Campbell, and E.C. Butcher. 2001. CC chemokine receptor (CCR)4 and the CCR10 ligand

cutaneous T cell–attracting chemokine (CTACK) in lymphocyte traffacking to inflamed skin. *J. Exp. Med.* 194:1541–1547. http://dx.doi.org/10.1084/jem.194.10.1541

Rott, L.S., J.R. Rosé, D. Bass, M.B. Williams, H.B. Greenberg, and E.C. Butcher. 1997. Expression of mucosal homing receptor alpha4beta7 by circulating CD4+ cells with memory for intestinal rotavirus. *J. Clin. Invest.* 100:1204–1208. http://dx.doi.org/10.1172/JCI119633

Sather, B.D., P. Treuting, N. Perdue, M. Miazgowicz, J.D. Fontenot, A.Y. Rudensky, and D.J. Campbell. 2007. Altering the distribution of Foxp3+ regulatory T cells results in tissue-specific inflammatory disease. *J. Exp. Med.* 204:1335–1347. http://dx.doi.org/10.1084/jem.20070081

Shang, L., N. Thirunarayanan, A. Viejo-Borbolla, A.P. Martin, M. Bogunovic, F. Marchesi, J.C. Unkeless, Y. Ho, G.C. Furtado, A. Alcami, et al. 2009. Expression of the chemokine binding protein M3 promotes marked changes in the accumulation of specific leukocytes subsets within the intestine. *Gastroenterology.* 137:1006–1018. http://dx.doi.org/10.1053/j.gastro.2009.05.055

Shankar, S.P., M.S. Wilson, J.A. DiVietro, M.M. Mentink-Kane, Z. Xie, T.A. Wynn, and K.M. Druey. 2012. RGS16 attenuates pulmonary Th2/Th17 inflammatory responses. *J. Immunol.* 188:6347–6356. http://dx.doi.org/10.4049/jimmunol.1103781

Sigmundsdottir, H., J. Pan, G.F. Debes, C. Alt, A. Habtezion, D. Soler, and E.C. Butcher. 2007. DCs metabolize sunlight-induced vitamin D3 to 'program' T cell attraction to the epidermal chemokine CCL27. *Nat. Immunol.* 8:285–293. http://dx.doi.org/10.1038/ni1433

Soler, D., T.L. Humphreys, S.M. Spinola, and J.J. Campbell. 2003. CCR4 versus CCR10 in human cutaneous TH lymphocyte trafficking. *Blood.* 101:1677–1682. http://dx.doi.org/10.1182/blood-2002-07-2348

Stagg, A.J., M.A. Kamm, and S.C. Knight. 2002. Intestinal dendritic cells increase T cell expression of alpha4beta7 integrin. *Eur. J. Immunol.* 32:

1445–1454. http://dx.doi.org/10.1002/1521-4141(200205)32:5<1445::AID-IMMU1445>3.0.CO;2-E

Stolberg, V.R., B.C. Chiu, B.M. Schmidt, S.L. Kunkel, M. Sandor, and S.W. Chensue. 2011. CC chemokine receptor 4 contributes to innate NK and chronic stage T helper cell recall responses during Mycobacterium bovis infection. *Am. J. Pathol.* 178:233–244. http://dx.doi.org/10.1016/j.ajpath.2010.11.036

Strutt, T.M., K.K. McKinstry, J.P. Dibble, C. Winchell, Y. Kuang, J.D. Curtis, G. Huston, R.W. Dutton, and S.L. Swain. 2010. Memory CD4+ T cells induce innate responses independently of pathogen. *Nat. Med.* 16:558–564. http://dx.doi.org/10.1038/nm.2142

Teijaro, J.R., D. Turner, Q. Pham, E.J. Wherry, L. Lefrançois, and D.L. Farber. 2011. Cutting edge: Tissue-retentive lung memory CD4 T cells mediate optimal protection to respiratory virus infection. *J. Immunol.* 187:5510–5514. http://dx.doi.org/10.4049/jimmunol.1102243

Thomas, P.G., S.A. Brown, W. Yue, J. So, R.J. Webby, and P.C. Doherty. 2006. An unexpected antibody response to an engineered influenza virus modifies CD8+ T cell responses. *Proc. Natl. Acad. Sci. USA.* 103:2764–2769. http://dx.doi.org/10.1073/pnas.0511185103

Thomas, S.Y., A. Banerji, B.D. Medoff, C.M. Lilly, and A.D. Luster. 2007. Multiple chemokine receptors, including CCR6 and CXCR3, regulate antigen-induced T cell homing to the human asthmatic airway. *J. Immunol.* 179:1901–1912.

Vermaelen, K.Y., I. Carro-Muino, B.N. Lambrecht, and R.A. Pauwels. 2001. Specific migratory dendritic cells rapidly transport antigen from the airways to the thoracic lymph nodes. *J. Exp. Med.* 193:51–60. http://dx.doi.org/10.1084/jem.193.1.51

von Wulffen, W., M. Steinmueller, S. Herold, L.M. Marsh, P. Bulau, W. Seeger, T. Welte, J. Lohmeyer, and U.A. Maus. 2007. Lung dendritic cells elicited by Fms–like tyrosine 3-kinase ligand amplify the lung inflammatory response to lipopolysaccharide. *Am. J. Respir. Crit. Care Med.* 176:892–901. http://dx.doi.org/10.1164/rccm.200608-1068OC